# Theoretical Study of the Adsorption of the Butanol Isomers in H-ZSM-5

Cuong M. Nguyen, Marie-Françoise Reyniers,* and Guy B. Marin

Laboratory for Chemical Technology, Ghent University, Krijgslaan 281 S5, B-9000 Gent, Belgium

Ⓢ *Supporting Information*

ABSTRACT: The adsorption of the four butanol isomers (1-BuOH, i-BuOH, 2-BuOH, and t-BuOH) at the Al12—O24-(H)—Si12 intersection site in H-ZSM-5 is investigated using the periodic [DFT-D] approach in which a damped interatomic potential (D) is included within the periodic density functional theory (pbcDFT) calculations to account for dispersive van der

Waals (vdW) interactions. Both the pbcDFT and pbc[DFT-D] methods yield largely similar results for the geometry of adsorbed complexes. The pbc[DFT-D] adsorption energies of the butanols are similar to those obtained using the pbcDFT with an add-on single-point dispersion-energy correction (pbcDFT + D). The adsorption strength of butanols decreases in the following order: 1-BuOH (-160 to -164 kJ mol^{-1}) > 2-BuOH (-155 to -157 kJ mol^{-1}) > t-BuOH (-151 kJ mol^{-1}) > i-BuOH (-147 kJ mol^{-1}). On the basis of a partial Hessian vibration analysis of the most stable physisorbed and chemisorbed complexes, reported experimental infrared (IR) spectra could be interpreted by assuming an equilibrium between physisorbed and chemisorbed minima on a flat potential energy surface. The extent to which the zeolite proton is transferred upon physisorption of the butanols increases from 1-BuOH to t-BuOH in agreement with an increase of the proton affinity of the alcohols. At the straight channel, the hydrogen bond strength ranges from -73 to -88 kJ mol^{-1} while at the zigzag channel, the hydrogen bond strength for 2-BuOH (-91 kJ mol^{-1}) is somewhat larger as compared to 1- and i-BuOH (-68 to -72 kJ mol^{-1}). Upon chemisorption, the four butoxonium ions experience similar Coulomb and hydrogen bonding interactions. Steric constraints and vdW interactions exerted by the zeolite frame are found to be the dominant factors in governing the adsorption strength of butanols in H-ZSM-5. At the straight channel, the steric constraints increase slightly by $+15$ kJ mol^{-1} in going from 1-BuOH to t-BuOH while in the zigzag channel a remarkably more pronounced increase of $+63$ kJ mol^{-1} is observed. Neither for physisorption nor for chemisorption of i-BuOH and t-BuOH, there is an energetic preference for one of the channels because in both channels vdW interactions counterbalance steric constraints. In contrast, for 1-BuOH and 2-BuOH vdW interactions prevail leading to an energetic preference of some $11-14$ kJ mol^{-1} for both physisorption and chemisorption in the zigzag channel. Accounting for the formation enthalpy of the gas-phase butanols, the stability of the adsorbed complexes of t-BuOH and 2-BuOH is predicted to be some $15-20$ kJ mol^{-1} higher than those of 1-BuOH and i-BuOH.
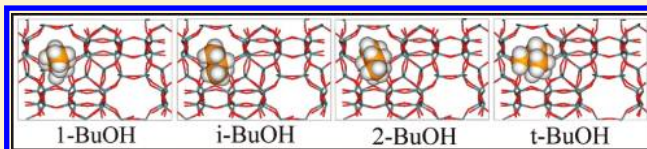
1. INTRODUCTION

Zeolites are among the most important industrial catalysts. The unique character of zeolitic molecular sieves originates from the uniform distribution of the active sites, Brønsted acid sites (BASs), in their micropores and cavities.[1] The catalytic behavior of the zeolite is therefore dependent both on the acidity and on the geometry and dimension of the zeolite framework, which govern the diffusion, sorption/desorption of both reactants and products inside the zeolite.[2] The reaction kinetics and product distribution are thus controlled by the whole zeolite framework to a significant extent.[2] Therefore, it is important to obtain more insight into the effect of the zeolite framework on reaction kinetics and thermodynamics.

Of increased recent interest is the conversion of renewable biomass-derived alcohols into gasoline, biofuels, and biochemicals to reduce society's dependence on fossil fuel.[3-5] To improve the efficiency of zeolite-catalyzed alcohol conversion processes, insight into the detailed reaction mechanism as well as accurate thermodynamic and kinetic parameters of the elementary reactions is of crucial importance. Up to date, however, detailed mechanistic studies of the intrazeolitic conversion of alcohols are still largely lacking and the elucidation of the reaction mechanism from experimental data only is extremely difficult. One of the main topics of debate is centered on the nature and stability of alcohol—zeolite adsorption complexes that are initially formed over the BASs in alcohol conversion processes.[6-17] Physisorbed and chemisorbed complexes are both stabilized by hydrogen bonding (HB) interactions (Figure 1) and differ in the extent to which the zeolite acid proton has been transferred to the alcohol.

A limited number of both experimental and theoretical works have indicated that in addition to acidity, also pore structure and dimensions of the zeolite are important factors in controlling the nature and stability of alcohol—zeolite complexes.[18-22] The effect of the zeolite framework is rather complicated and is executed through steric constraints and/or dispersive vdW
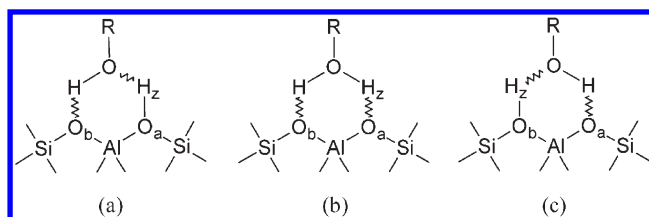
Figure 1. Alcohol—zeolite interaction. Hydrogen bonded physisorbed (a,c) and protonated chemisorbed complex (b) over the Brønsted acid site (BAS). H_z, zeolite proton; O_a, O24; O_b, O20; and Al, Al12.

interactions.[23] In a comprehensive first principles molecular dynamics (MD) study of methanol adsorbed in several different zeolites, Stich et al.[24] suggested that the proton transfer is strongly correlated with steric constraints and vdW interactions exerted by the zeolite framework. There is a noticeable increase in the fraction of chemisorbed methanol with decreasing channel diameter of the zeolite framework. Unfortunately, no quantitative correlation was found between the methanol adsorption energy and the dimension of these zeolite frameworks.[21,24] Very recently, Nguyen et al.[25] employed periodic density functional theory with a single-point dispersion-energy correction (pbcDFT + D) to study the adsorption of C1—C4 primary alcohols in H-ZSM-5. The vdW interactions due to the zeolite frame are found to contribute significantly to the adsorption energies of the alcohols and increase linearly with ca. 15 kJ mol^{-1} per carbon atom,[25] which is in agreement with experimental result.[26]

To elucidate the influence of shape selectivity and pore structure of H-ZSM-5 on the adsorption and dehydration kinetics of the four butanols, Zamaraev et al.[27−31] carried out a series of experimental studies using a combination of in situ FT-IR spectroscopy and gas chromatography. The IR spectra of the adsorbed alcohols are characterized by two broad OH bands at 2400—2450 and 1500—1600 cm^{-1}, which are involved in strong hydrogen-bonding complexes.[27−31] However, whether these complexes are physisorbed or chemisorbed over the BAS of H-ZSM-5 remains unclear in the works by Zamaraev et al.[27−31] Note that the highest frequency OH bands at 3500—3700 cm^{-1} are reported for i-BuOH-H-ZSM-5[30] and t-BuOH-HZSM-5[31] only. Interpretation of the IR spectra of absorbed butanols is hampered due to their fast dehydration to the corresponding butenes.[27−31] In particular, upon adsorption of 2-BuOH[28] and t-BuOH,[31] dehydration can be expected to proceed even at moderate temperatures and the concomitant formation of adsorbed water, characterized by one bending at 1640 cm^{-1} and one stretching at 3700 cm^{-1}, complicates the assignment of frequencies in these regions. To complement the aforementioned experimental works, Zamaraev et al.[32] performed simulations of the adsorption of the four butanols in H-ZSM-5 and silicalite, using an molecular mechanics energy minimization procedure supplemented by a Monte Carlo/molecular dynamic (MC/MD) algorithm to assist in the location of minima. At a number of different crystallographic positions, adsorption energies of the four butanols ranging from −114 to −132 in H-ZSM-5 and from −120 to −138 kJ mol^{-1} in silicalite were obtained. Also, the O_a—H_z bond length in H-ZSM-5 was found to remain unchanged upon adsorption of the butanols, indicating no specific interaction (HB and/or Coulomb) between the butanols and the BAS.[32] Clearly, these results indicate that the energy minimization procedure supplemented by a MC/MD algorithm is less suited to provide an accurate description of

alcohol adsorption in zeolites where both bonded and dispersive vdW interactions play important stabilizing roles.

As an extension of our previous pbcDFT + D study on C1—C4 primary alcohols,[25] the present work investigates the effect of the pore dimensions of H-ZSM-5 on the energetics of adsorption of the four butanol isomers, that is, 1-BuOH, i-BuOH, 2-BuOH, and t-BuOH. These alcohols are ideally suited to examine the H-ZSM-5 framework effects since (1) their dimensions are comparable to those of the H-ZSM-5 channels and (2) their hydrocarbon skeletons with different branching present a convenient testing group to explore the role of the molecular shape and structure in controlling the nature and stability of the adsorbed complexes. Because of the dominant stabilizing role of vdW interactions, the pbc[DFT-D] approach[33,34] in which the Grimme's dispersion correction[33] is included in the periodic DFT calculations[34] is used in the present work for obtaining optimized structures, energies, and for determining harmonic vibrational frequencies of the adsorbed systems.

2. MODELS AND METHODS

2.1. Silicalite and H-ZSM-5 Models. Orthorhombic H-ZSM-5 (HAlSi$_{95}$O$_{192}$) and its siliceous analogue silicalite (Si$_{96}$O$_{192}$) unit cells[25] are utilized as adsorbents for the docking of the four butanols. The orthorhombic ZSM-5 unit cell has 12 crystallographically distinguishable tetrahedral framework sites (T sites) for Si/Al substitution. Experimental works[35,36] show a variability of the Al siting for ZSM-5 samples with the Si/Al ratio of 95 (one Al per unit cell). However, performing calculations for adsorption of the four butanols on all the different possible T sites is computationally very expensive and practically unfeasible. Besides, previous theoretical calculations report small differences in energy among structures with Al at different T sites.[37,38] For ZSM-5 samples with low Si/Al ratios (Si/Al < 45), that is, more than 2 Al per unit cell, the distribution of aluminum atoms exhibits insignificant effect on the acid strength of the zeolites.[39] Therefore, we select the "intersection" site Al12—O24(H)—Si12 to represent the Brønsted acid site because it is considered among the most stable sites for Al substitution[38,40,41] and has been chosen as the active site for several reactions.[24,25,41−43] Moreover, the intersection site provides maximum reaction space and easy access for reactants, especially bulky ones.[43,44] Considering the proton jump among the adjacent Al-bound oxygen atoms at the T-12 site, Svelle et al.,[22] and Nguyen et al.[25] found a energetic preference of 5—12 kJ mol^{-1} for the location of zeolite proton at the Al12—O20(H)—Si3 as compared with the Al12—O24(H)—Si12 bridging site. However, Nguyen et al.[25] have shown that the location of the zeolite proton at either of the two sites has no significant effect on the adsorption energy of alcohols.[22,25]

Structural parameters and graphical illustrations of the optimized silicalite and H-ZSM-5 unit cells are presented in our previous work.[25] In the present study, the notations $O_bAl[O_aH_z]$ and $O_aAl[O_bH_z]$ are used to indicate the location of the zeolite proton (H_z) at O24 (O_a) and O20 (O_b) of the Al12 site, respectively (Figure 1). Geometries of the representative i-BuOH-silicalite physisorbed complexes as well as i-BuOH-H-ZSM-5 physisorbed and chemisorbed complexes over the intersection site $O_bAl[O_aH_z]$ are illustrated in Figures 2—4. Those of the other butanols are given in the Supporting Information (S.1-S.3).

In addition, BuOH-HZSM-5 physisorbed complexes are sampled at the other BAS $O_aAl[O_bH_z]$ with the zeolite proton
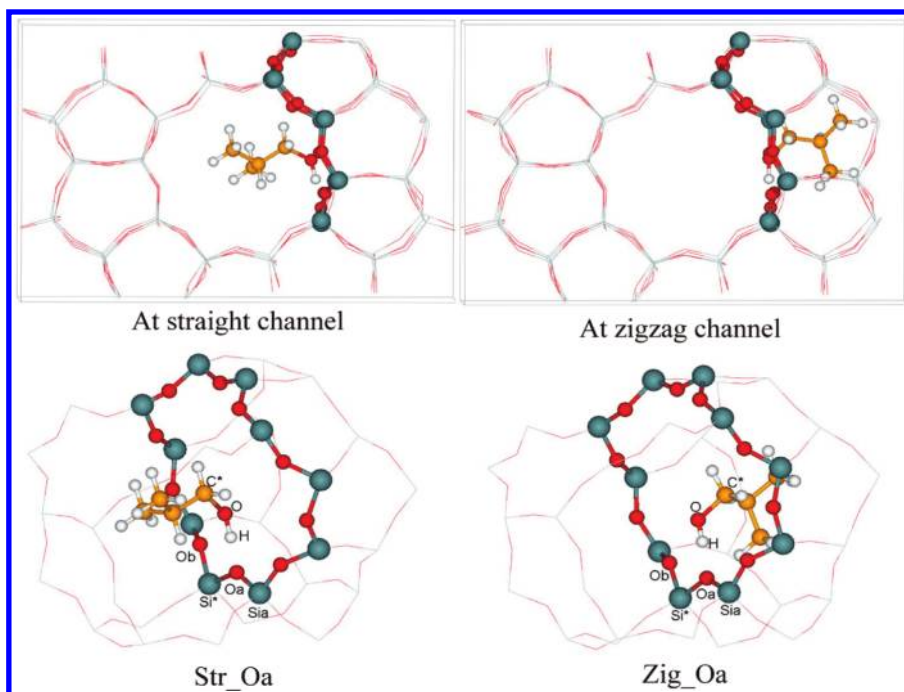
Figure 2. Representative silicalite-BuOH physisorbed complexes. i-C_4H_9OH physisorption at the straight and zigzag channels viewed in the [010] direction (top panels). Highlighted atoms define the 10-T intercrossing ring between the two channels. $Si^* - O_a - Si_a$ indicates the T12 bridging position Si12−O24−Si12 for Al substitution at Si* with Si* = Si12, O_a = O24, Si_a = Si12, respectively. The intersection space between two channels (top pannel) is divided into two parts by the 10-T ring; the left part belongs to the straight channel while the right part belongs two the zigzag channel. The i-BuOH molecule has the H atom pointed to O_a and the hydrocarbon chain accommodated at the straight (Str_O_a) or zigzag channel (Zig_O_a). Code colors used: oxygen (red), silicon (gray), hydrogen (white), and carbon (yellow).
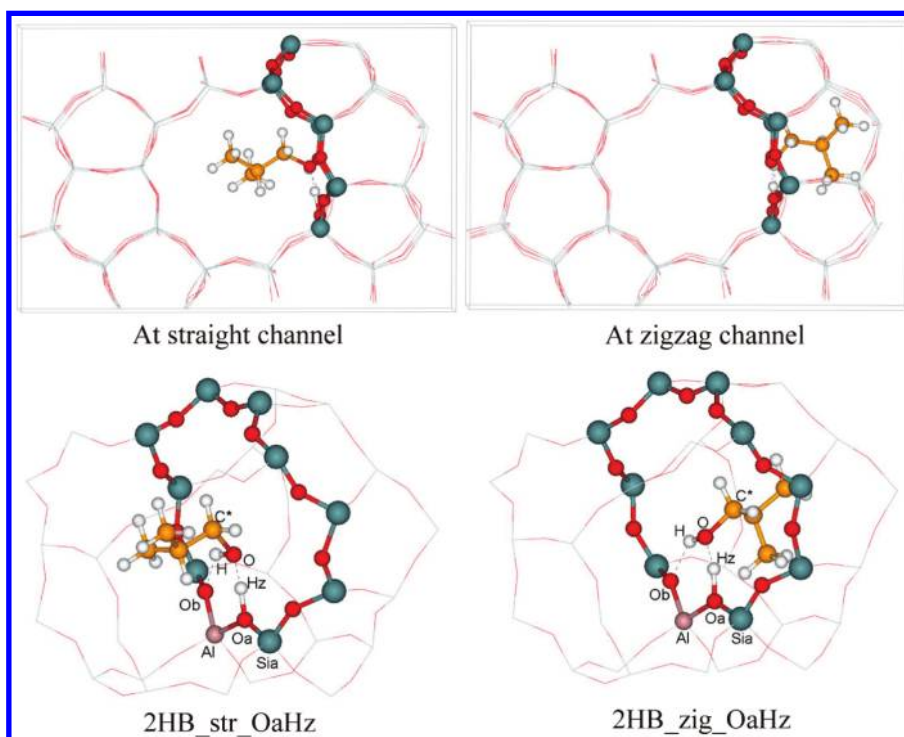
Figure 3. Representative H-ZSM-5-BuOH physisorbed complexes at the $O_bAl[O_aH_z]$. i-BuOH physisorption at the straight (str) and zigzag (zig) channels viewed in the [010] direction (top pannels). Highlighted atoms define the 10-T intercrossing ring between the two channels. Si_a = Si12, O_a = O24, Al = Al12, and O_b = O20. The alcohol molecule interacts with the BAS via two hydrogen bonds O---H_z and O_b---H (2HB_str_O_aH_z and 2HB_zig_O_aH_z). Code colors used: aluminum (pink), oxygen (red), silicon (gray), hydrogen (white), carbon (yellow).
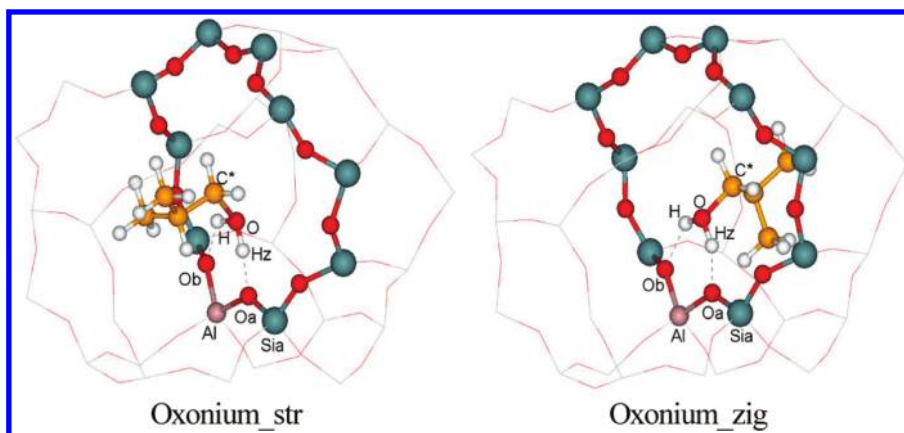
Figure 4. Representative H-ZSM-5-i-BuOH chemisorbed complexes. Oxonium_str at the straight channel and Oxonium_zig at the zigzag channel.

attached to O_b. For all butanols except 2-BuOH at the zigzag channel, the location of the zeolite proton (H_z) at O_a or O_b has no significant effect on the structural parameters and energetics of the physisorbed complexes. Detailed geometrical parameters and physisorption energies of the butanols over the BAS O_aAl-$[O_bH_z]$ are presented in the Supporting Information (S.4).

2.2. Computational Methods. In this study, both the pbcDFT and pbc[DFT-D][33,34] approaches were utilized for obtaining optimized structures, energies of the four butanols adsorbed in silicalite and H-ZSM-5. Harmonic vibrational modes of gas-phase alcohols, unloaded H-ZSM-5, and adsorption complexes were calculated. For periodic structures, Partial Hessian Vibrational Analysis (PHVA) was performed for only AlO_3OH and four Al-bound adjacent SiO_4 tetrahedral groups in addition to the adsorbate (in the case of adsorbed complexes) to avoid the computational cost for the whole systems of up to 304 atoms. For gas-phase alcohols, the full Hessian was calculated. Bader charge analysis[45] was utilized to calculate formal charge of adsorbed fragments.

Also, optimized geometries obtained using the pbcDFT level of theory were subject to a single-point dispersion-energy correction calculation (pbcDFT + D) to pragmatically account for the contribution of dispersive vdW interactions to the total adsorption energy of alcohols. The dispersion-corrected energies obtained using both the pbcDFT + D and pbc[DFT-D] approaches were then compared.

Physisorption or chemisorption energy (ΔE_{phys} or ΔE_{chem}, respectively) of an alcohol in silicalite/H-ZSM-5 is computed relative to the unloaded silicalite/H-ZSM-5 and the corresponding gas phase alcohol at 0 K. The proton transfer energy, ΔE_{pt}, is defined as the dispersion-corrected energy difference between chemisorbed and physisorbed complex.

The effect of the O−H bond length variation on the energy and on the harmonic stretching frequencies of the H_z−O−H group of the chemisorbed complexes was inspected for 1-BuOH at the zigzag channel and for t-BuOH at the straight channel.

2.2.1. pbcDFT Calculations. Periodic DFT calculations are performed using the Vienna Ab Initio Simulation Package (VASP) code.[46] The Kohn−Sham equations were solved variationally using the projector-augmented wave (PAW) method[47,48] and gradient-corrected Perdew−Burke−Ernzerhof (PBE) exchange-correlation functional.[49] Brillouin zone sampling was restricted to the Γ point. For the geometry optimization, a plane-wave cutoff of 400 eV was employed and the convergence criterion for the electronic self-consistency loop was set to 10^{-5} eV.

Structures were considered converged when forces on all atoms dropped below 0.05 eV/Å. Tests of increasing plane-wave cutoff to 600 eV and decreasing electronic threshold to 10^{-6} eV proved that values used were sufficient to converge energy differences for alcohol−zeolite systems within 2 kJ mol^{-1}. The force threshold of 0.05 eV/Å was verified to be sufficient to obtain reliable eigenfrequencies of alcohol−zeolite complexes.

2.2.2. pbc[DFT-D] Calculations. The pbc[DFT-D] approach for periodic systems according to Kerber et al.[33] using the Ewald summation technique[50] was used to implement Grimme's dispersion correction[34] within VASP[46] for the zeolite. The total dispersion-corrected energy of a periodic system is thus defined as

$$E_{DFT-D} = E_{DFT} + E_D \qquad (1)$$

where E_{DFT} is the self-consistent DFT Kohn−Sham electronic energy and E_D is the empirical dispersion energy. Calculation of the dispersion energy term for periodic systems involves the evaluation of lattice sums of the form

$$E_D = -\frac{s_6}{2} \sum_{L} \sum_{i,j \,\in\, L=0} \frac{\sqrt{c_6^i c_6^j}}{|r_{ij} - L|^6} f_D(|r_{ij} - L|) \qquad (2)$$

in which s_6 is the global scaling factor, 0.75 is for PBE functional, L is the direct lattice translation vector, i and j are the atoms within the central unit cell, c_6^i denotes the atomic dispersion coefficients, and f_D is a damping function of interatomic distance r_{ij}. The sums over i and j go over all atoms inside the cell except that $i \neq j$ when $L = 0$. Detailed information over the calculation technique for the lattice sums of dispersion energy as well as the implementation of pbc[DFT-D] is outlined in the work by Kerber et al.[33] All the atomic parameters and the form of damping function are given by Grimme et al.[34]

A detailed comparison of the performance of pbcDFT + D versus pbc[DFT-D] with respect to geometries, adsorption energies and vibrational motions of the four butanols adsorbed in silicalite and H-ZSM-5 is presented in the Supporting Information (S.5). Both the pbcDFT and pbc[DFT-D] methods yielded largely similar results for the geometry optimization and PHVA analysis. As expected, the adsorption energies obtained using the pbcDFT are dramatically underestimated. Both the pbcDFT + D and pbc[DFT-D] approaches overcome this shortcoming of the pbcDFT. An agreement is observed between

the two approaches for computing the DFT and D energy terms of the total dispersion-corrected adsorption energy.

The geometry optimization and energy calculation results show that both the pbcDFT + D and pbc[DFT-D] approaches offer an improvement to the pbcDFT approach in modeling the adsorption of alcohols in zeolite where the dispersive vdW interactions play a significant role in governing the stability of adsorbed complexes. Furthermore, together with the Hessian analysis and transition state finding algorithms integrated in VASP, the pbc[DFT-D] approach provides a comprehensive simulation methodology, that is, all geometrical, energetic, and energy derivative calculations are performed at the same level of pbc[DFT-D] theory, for both thermodynamic and kinetic study of chemical reactions in periodic structures such as zeolites. The following sections present a discussion of the structural effects of the MFI framework of silicalite and H-ZSM-5 on the adsorption of the four butanols according to pbc[DFT-D] results.

3. RESULTS AND DISCUSSION

3.1. Physisorption in Silicalite. *3.1.1. Geometry.* Upon adsorption at both the straight and zigzag channels of silicalite,

Table 1. Geometrical Parameters (pm)[a] of Butanols Physisorbed in Silicalite Obtained Using the pbc[DFT-D] Approach

		gas-phase		in silicalite	
		H$-$O	PA[b]	H$-$O	H---O$_a$
straight channel	1-BuOH	97.3	-834	97.4	214.1
	i-BuOH	97.2	-836	97.6	216.2
	2-BuOH	97.4	-849	97.4	228.5
	t-BuOH	97.5	-860	97.6	214.4
zigzag channel	1-BuOH			97.4	226.8
	i-BuOH			97.5	238.2
	2-BuOH			97.6	210.7
	t-BuOH			97.6	210.9

[a] Atom labels are defined in Figure 2. [b] Gas-phase proton affinities at 0 K (PA, kJ mol^{-1}) of butanols were measured using Gaussian at the CBS-QB3 level of theory.

there are no significant changes in structure of the alcohols, namely, the alcohol OH bond is elongated by only 0.0$-$0.4 pm (Table 1), which is in agreement with the observation for the C1$-$C4 primary alcohols physisorbed in silicalite using the pbcDFT for geometry optimization.[25] The weak and nonspecific interaction between one oxygen of the zeolite lattice (O$_a$) and the hydroxyl hydrogen (H) of the butanols (Figure 2) is clearly demonstrated by the long interatomic distances d[H---O$_a$] of 210.7$-$238.2 pm.

3.1.2. Physisorption Energy. Table 2 presents physisorption energies of the four butanols. At the straight channel, all butanols have insignificantly different ΔE_{DFT-D} while a wider range of ΔE_{DFT-D} is observed at the zigzag channel. At both the channels, the BuOH-silicalite complexes are mainly stabilized by the prevailing vdW dispersive interactions due to the surrounding silicalite lattice (see ΔE_D and %ΔE_D, Table 2).

Further analysis of ΔE_{DFT} and ΔE_D contributions allows the evaluation of the role of the molecular shape and structure in governing the physisorption strength of the butanols in silicalite. In going from 1-BuOH to t-BuOH, the ΔE_{DFT} strength decreases slightly from -14 to 1 kJ mol^{-1} at the straight channel, but more remarkably from -4 to $+59$ kJmol^{-1} at the zigzag channel (Table 2) indicating an increase in steric constraints with increasing branching level and bulkiness of the hydrocarbon chain. Taking 1-BuOH as a reference, the destabilization due to steric constraints at the straight or zigzag channel, E_{strain}, upon adsorption of another butanol can be estimated as the difference in their ΔE_{DFT} (see E_{strain}, Table 2). The largest E_{strain} of $+63$ kJ mol^{-1} is estimated for adsorption of t-BuOH, the bulkiest butanol, at the zigzag channel. At the straight channel, the slight increase in E_{strain} in going from 1-BuOH to t-BuOH is partly counteracted by a small increase in ΔE_D resulting in largely similar ΔE_{DFT-D} of the four butanols. However, at the zigzag channel, the former factor prevails and renders the adsorption of t-BuOH some 20$-$30 kJ mol^{-1} less energetically favorable than that of other butanols.

Table 3 presents the difference in adsorption energy computed between the two channels of silicalite ($\delta_{ch} = \Delta E_{phys}^{zigzag} - \Delta E_{phys}^{straight}$) and allows the evaluation of the pore dimension effect. According to $\delta_{ch}[\Delta E_{DFT-D}]$, the zigzag channel is energetically somewhat more favorable than the straight channel for

Table 2. DFT-D, DFT, and D Physisorption Energies (ΔE_{phys}, kJ mol^{-1}) of Butanols in Silicalite and H-ZSM-5 Obtained Using the pbc[DFT-D] Approach

		in silicalite						in H-ZSM-5					$\delta[\Delta E_{DFT}]^d$
		ΔE_{DFT-D}	ΔE_{DFT}	ΔE_D	%ΔE_D	E_{strain}^b	$\Delta E_{MC/MD}^c$	ΔE_{DFT-D}	ΔE_{DFT}	ΔE_D	%ΔE_D	$\Delta E_{MC/MD}^c$	
straight channel	1-BuOH	-68	-14	-54	79	0	$-116/-117$	-148	-87	-61	41	$-115/-120$	-73
	i-BuOH	-66	-10	-56	85	$+4$	$-109/-121$	-147	-89	-58	40	-120	-79
	2-BuOH	-58	-2	-56	97	$+12$	$-106/-112$	-144	-81	-63	44	$-113/-127$	-83
	t-BuOH	-60	1	-61	102	$+15$	$-110/-114$	-148	-87	-61	41	$-117/-124$	-88
zigzag channel	1-BuOH	-79	-4	-75	95	0	$-117/-132$	-160	-76	-84	53	$-120/-138$	-72
	i-BuOH	-71	20	-91	128	$+24$	$-108/-120$	-147	-48	-99	67	$-115/-119$	-68
	2-BuOH	-70	33	-103	147	$+37$	$-100/-118$	-155	-58	-97	63	$-109/-127$	-91
	t-BuOH[a]	-51	59	-110	216	$+63$	$-109/-114$					$-111/-129$	

[a] Physisorbed complex of t-BuOH could not be located at the zigzag channel of H-ZSM-5. [b] Steric constraints energy (E_{strain}) is calculated as the increase in ΔE_{DFT} endothermicity of the other butanols relative to 1-BuOH at each channel of silicalite. E_{strain} of 1-BuOH is assumed to be zero. [c] Physisorption energies (kJ mol^{-1}) of butanols at different crystallographic positions in silicalite and in H-ZSM-5 obtained using the energy minimization procedure supplemented by a Monte Carlo/molecular dynamics (MC/MD) algorithm taken from ref 32. [d] $\delta[\Delta E_{DFT}] = \Delta E_{DFT/H-ZSM-5} - \Delta E_{DFT/silicalite}$ used as a rough estimate of hydrogen bond strength between the butanol and the BAS of H-ZSM-5.

8662

dx.doi.org/10.1021/jp111698b |*J. Phys. Chem. C* 2011, 115, 8658–8669

Table 3. The Difference (δ_{ch}, kJ mol^{-1} = $\Delta E_{phys}^{zigzag} - \Delta E_{phys}^{straight}$) in Physisorption Energy Computed between the Zigzag and Straight Channel Obtained Using the pbc[DFT-D] Approach

	in silicalite			in H-ZSM-5		
	$\delta_{ch}[\Delta E_{DFT-D}]$	$\delta_{ch}[\Delta E_{DFT}]$	$\delta_{ch}[\Delta E_D]$	$\delta_{ch}[\Delta E_{DFT-D}]$	$\delta_{ch}[\Delta E_{DFT}]$	$\delta_{ch}[\Delta E_D]$
1-BuOH	−11	+10	−21	−12	+11	−23
i-BuOH	−6	+30	−36	0	+41	−41
2-BuOH	−11	+36	−47	−11	+23	−34
t-BuOH[a]	+9	+58	−49			

[a] Physisorbed complex of t-BuOH could not be located at the zigzag channel of H-ZSM-5.

Table 4. Geometrical Parameters (Distances in pm and Angles in Degrees)[a] of Unloaded H-ZSM-5 and Physisorbed BuOH-H-ZSM-5 Complexes at the Straight and Zigzag Channels Using the pbc[DFT-D] Approach

		H_z-O_a	$H-O$	H_z---O	H---O_b	q^b	Si_a-O_a	Si_b-O_b	$Al-O_a$	$Al-O_b$	O_aAlO_b	Si_aO_aAl	Si_bO_bAl
Unloaded H-ZSM-5		97.7					170.6	161.0	191.1	172.7	96.8	135.5	143.2
Physisorbed													
straight channel	1-BuOH	113.9	98.5	130.4	211.7	0.11	166.0	161.1	184.8	175.0	99.1	134.3	143.0
	i-BuOH	117.2	99.0	126.3	203.0	0.12	165.4	161.4	183.9	175.6	99.3	134.8	142.9
	2-BuOH	128.1	99.9	116.6	194.9	0.13	164.4	161.7	182.5	176.4	100.2	135.7	140.6
	t-BuOH	130.6	99.7	114.2	194.8	0.14	163.7	161.7	181.6	176.8	99.8	136.5	140.1
zigzag channel	1-BuOH	117.5	99.3	125.6	191.3	0.13	165.5	161.5	184.3	176.2	99.9	134.9	141.8
	i-BuOH	119.7	99.5	124.4	189.5	0.12	165.2	161.6	184.0	176.2	98.8	133.1	141.7
	2-BuOH	126.3	99.4	117.6	196.3	0.12	164.3	161.4	182.7	176.4	99.3	135.3	140.4

[a] Atom labels are defined in Figure 3. [b] q: formal charge of the physisorbed butanol molecule.

the adsorption of 1-BuOH, i-BOH, and 2-BuOH owing to the predominance of the vdW interactions over the steric constraints ($\delta_{ch}[\Delta E_D] = -21$ to -47 kJ mol^{-1} versus $\delta_{ch}[\Delta E_{DFT}] = +10$ to $+36$ kJ mol^{-1}). Adsorption of the bulkiest t-BuOH is, however, slightly preferred at the more extended straight channel since the former cannot counterbalance the latter factor ($\delta_{ch}[\Delta E_D] = -49$ kJ mol^{-1} versus $\delta_{ch}[\Delta E_{DFT}] = +58$ kJ mol^{-1}). Taking the most stable physisorbed complex of each BuOH, the DFT-D physisorption strength decreases in the order: 1-BuOH (-79 kJ mol^{-1}) > i-BuOH (-71 kJ mol^{-1}) $\approx$ 2-BuOH (-70 kJ mol^{-1}) > t-BuOH (-60 kJ mol^{-1}).

3.2. Physisorption in H-ZSM-5. *3.2.1. Geometry.* In contrast to the alcohol-silicalite complexes, all alcohol-H-ZSM-5 physisorbed complexes are characterized by two distinguishable HBs: a primary H_z---O HB between the zeolite hydrogen and the oxygen of the alcohol and a secondary H---O_b HB between the alcohol hydrogen and the adjacent alumina-bound oxygen (Table 4). All the physisorbed butanols possess a small positive charge (q) in the range $+0.11$ to $+0.14$.

It is observed at both the straight and zigzag channels of H-ZSM-5 that the extent to which the zeolite proton H_z is partially transferred to the alcohol molecule increases in going from 1-BuOH over i-BuOH to 2-BuOH and t-BuOH as clearly evidenced by the increase in H_z-O_a bond length and the decrease in H_z---O distance (Table 4). Further, the 2-HB physisorbed complex of t-BuOH could not be located at the zigzag channel; all geometrical optimizations starting from a physisorbed or a chemisorbed initial geometry relaxed to the protonated oxonium as the local minimum. A first principles molecular dynamic study of methanol adsorption in several zeolite frameworks[24] showed that there is a noticeable increase

in the fraction of chemisorbed methanol with decreasing free space available for relaxation of the adsorbed methanol molecule. Therefore, it is probable that the confined zigzag channel is not preferable for the formation of 2-HB physisorbed complex of the bulky t-BuOH. Upon physisorption of the butanols, changes of other structural parameters of the H-ZSM-5 framework are also induced at both the channels (Table 4). It is interesting to note that the extent of these framework distortions in going from 1-BuOH to t-BuOH parallels the extent of partial proton transfer as discussed above.

The marked differences in $d[H_z-O_a]$ and $d[H_z$---$O]$ observed between 1-BuOH and t-BuOH at the straight channel may be ascribed to the intrinsic basicity of the alcohol, measured by its gas phase proton affinity (PA). Because of the discrepancy among the reported PA values for the butanols in literature (see Supporting Information S6),[51−55] PAs of the four BuOH isomers were calculated at the CBS-QB3 level of theory using Gaussian (see Table 1). The calculated PAs steadily increase in going from 1-BuOH over i-BuOH and 2-BuOH to t-BuOH indicating an increase in the strength of the HB between the BAS and the BuOH molecule, resulting in an enhancement of the partial proton transfer from the zeolite.

3.2.2. Physisorption Energy. The ΔE_{DFT-D} of the four butanols in H-ZSM-5 is similar at the straight channel but slightly different at the zigzag channel (Table 2).

At the straight channel, all butanols have virtually identical ΔE_{DFT} and also indifferent ΔE_D. Assuming the similar steric constraints upon adsorption in H-ZSM-5 and in silicalite, the difference ($\delta[\Delta E_{DFT}]$) between $\Delta E_{DFT/H-ZSM-5}$ and $\Delta E_{DFT/silicalite}$ can be used as a rough estimate of the HB strength for the physisorbed butanols. At the straight channel, the HB strength

Table 5. Geometrical Parameters (pm)^a and Formal Charges of Butanols Chemisorbed at the Straight and Zigzag Channels of H-ZSM-5 Obtained Using the pbc[DFT-D] Approach

		H_z---O_a	H---O_b	H_z−O	H−O	q^b	$q(O_a)^b$	$q(O_b)^b$
straight channel	1-butoxonium	153.2	146.7	105.0	106.9	+0.77	−1.56	−1.55
	i-butoxonium	155.6	147.6	104.2	106.6	+0.78	−1.55	−1.55
	2-butoxonium	154.3	156.8	104.9	104.5	+0.78	−1.56	−1.56
	t-butoxonium	164.4	149.0	103.0	106.2	+0.80	−1.57	−1.55
	t-butoxonium_sym^c	152.5	157.8	105.1	104.0	+0.81	−1.57	−1.55
zigzag channel	1-butoxonium	145.5	155.5	107.0	104.4	+0.78	−1.55	−1.56
	1-butoxonium_sym^c	149.1	152.5	106.0	105.2	+0.77	−1.55	−1.56
	i-butoxonium	145.0	155.6	107.1	104.3	+0.76	−1.55	−1.55
	2-butoxonium	153.0	153.7	104.6	104.8	+0.78	−1.55	−1.57
	t-butoxonium	155.0	149.7	104.2	105.4	+0.76	−1.55	−1.55

^{a} Atom labels are defined in Figure 4. ^{b} q, $q(O_a)$, and $q(O_b)$: formal charge of the protonated $C_4H_9OH_2^+$ ion, O_a, and O_b, respectively. ^{c} Chemisorbed complexes with more symmetric OH covalent bond length.

Table 6. Geometrical Parameters (Distances in pm and Angles in Degree)^a of the Loaded H-ZSM-5 upon Chemisorption of Butanols at the Straight and Zigzag Channels Obtained Using the pbc[DFT-D] approach

		Si_a−O_a	Si_b−O_b	Al−O_a	Al−O_b	O_aAlO_b	$Si_a O_a$Al	$Si_b O_b$Al
Unloaded H-ZSM-5		170.6	161.0	191.1	172.7	96.8	135.5	143.2
Chemisorbed								
straight channel	1-butoxonium	162.4	163.6	178.9	180.5	98.8	138.4	138.4
	i-butoxonium	162.3	163.5	179.0	180.5	99.4	135.1	135.1
	2-butoxonium	162.4	162.8	179.3	179.4	99.7	139.5	139.5
	t-butoxonium	162.1	163.1	178.3	180.1	100.8	136.6	136.6
	t-butoxonium_sym	162.4	162.8	179.3	179.4	100.1	137.4	137.4
zigzag channel	1-butoxonium	162.7	162.9	180.1	179.6	98.6	136.0	136.0
	1butoxonium_sym	162.5	162.9	179.6	179.6	98.5	135.8	135.8
	i-butoxonium	162.8	162.9	179.9	179.7	99.8	137.3	137.3
	2-butoxonium	162.4	162.8	179.3	179.9	99.3	135.4	135.4
	t-butoxonium	162.6	162.8	179.8	180.2	100.1	135.6	135.6

^{a} Atom labels are defined in Figure 4.

ranges from −73 to −88 kJ mol^{-1} (see $\delta[\Delta E_{DFT}]$, Table 2) in line with the increase in PA in going from 1-BuOH to t-BuOH.

At the zigzag channel, a significantly larger ΔE_{DFT} is calculated for 1-BuOH in comparison with 2-BuOH and i-BuOH. The HB strength for 2-BuOH is however estimated to be somewhat larger as compared to 1-BuOH and i-BuOH (see $\delta[\Delta E_{DFT}]$, Table 2) in agreement with the extent of partial proton transfer as mentioned above. Therefore, the less exothermic ΔE_{DFT} of 2-BuOH and i-BuOH as compared with that of 1-BuOH is ascribed to the pronounced increase in E_{strain} of +37 kJ mol^{-1} in going from 1-BuOH to 2-BuOH. Also, the predominance of E_{strain} over HB and vdW interactions renders the ΔE_{DFT-D} of i-BuOH and 2-BuOH some 5−10 kJ mol^{-1} less exothermic than that of 1-BuOH (Table 2).

The channel preference for the adsorption of butanols, as indicated by $\delta_{ch}(\Delta E_{DFT-D})$ in Table 3, can be rationalized as a result of a subtle interplay between steric constraints and vdW interactions. Adsorption of 1-BuOH and 2-BuOH is energetically favorable at the compact zigzag channel while i-BuOH is equally preferred at both channels. Note also that the physisorption of t-BuOH is exclusive at the straight channel. Taking the most stable adsorbed complex of each BuOH, the ΔE_{DFT-D} strength decreases

in the order 1-BuOH (−160 kJ mol^{-1}) > 2-BuOH (−155 kJ mol^{-1}) > t-BuOH (−148 kJ mol^{-1}) ≈ i-BuOH (−147 kJ mol^{-1}).

The pbc[DFT-D] calculations predict significantly different ranges of adsorption energy for H-ZSM-5 and silicalite (−144 to −160 vs −51 to −79 kJ mol^{-1}), which is in agreement with −113 to −161 versus −33 to −83 vs kJ mol^{-1} computed for the C1−C4 primary alcohols by Nguyen et al[25] using the pbcDFT + D approach. In the calculations by Zamaraev et al.,[32] the magnitude of H-ZSM-5-alcohol and silicalite-alcohol interactions was however found to be largely identical (−100 to −132 versus −109 to −138 kJ mol^{-1}, Table 2). While no experimental adsorption enthalpy for the butanols has been reported, a significant difference of 55−60 kJ mol^{-1} in favor of H-ZSM-5 against silicalite for the adsorption enthalpy of methanol, ethanol, and 1-propanol is observed in the experimental study reported by Lee et al.[26] The results reported by Zamaraev et al.[32] seem to indicate that the energy minimization procedure supplemented by a MC/MD algorithm is less suited for the description of the alcohol−zeolite interactions.

3.3. Chemisorption. *3.3.1. Geometry.* All chemisorbed complexes are characterized by two largely indifferent HBs and two almost equivalent covalent OH bonds (Table 5). Moreover, the

8664

dx.doi.org/10.1021/jp111698b |*J. Phys. Chem. C* 2011, 115, 8658−8669

Table 7. Chemisorption Energies (ΔE_{chem}, kJ mol^{-1}), DFT-D Proton Transfer Energies (ΔE_{pt}, kJ mol^{-1}) and Iron Pair Interaction Energies (IP, kJ mol^{-1}) of Butanols in H-ZSM-5 Obtained Using the pbc[DFT-D] Approach (IP$_{DFT-D}$ = ΔE_{DFT-D} − DP^a − PA, IP$_{DFT}$ = ΔE_{DFT} − DP^a − PA, and IP$_D$ = IP$_{DFT-D}$ − IP$_{DFT}$)

		ΔE_{chem}				IP		
		ΔE_{DFT-D}	ΔE_{DFT}	ΔE_D	$\Delta E_{pt,\ DFT-D}$	IP$_{DFT-D}$	IP$_{DFT}$	IP$_D$
straight channel	1-butoxonium	−150	−84	−66	−2	−552	−486	−66
	i-butoxonium	−147	−88	−59	0	−547	−488	−59
	2-butoxonium	−146	−88	−58	−1	−533	−475	−58
	t-butoxonium	−150	−86	−64	−2	−526	−462	−64
	t-butoxonium_sym	−151	−88	−63	−3	−527	−464	−63
zigzag channel	1-butoxonium	−164	−79	−85	−4	−566	−481	−85
	1-butoxonium_sym	−163	−81	−82	−3	−565	−483	−82
	i-butoxonium	−146	−51	−95	+1	−546	−451	−95
	2-butoxonium	−157	−61	−96	−2	−544	−448	−96
	t-butoxonium	−148	−45	−103		−524	−421	−103

^{a} DP: Calculated deprotonation energy (1236 kJ mol^{-1}) of the acid site Al12−O24(H)Si12 of H-ZSM-5 taken from ref 56.
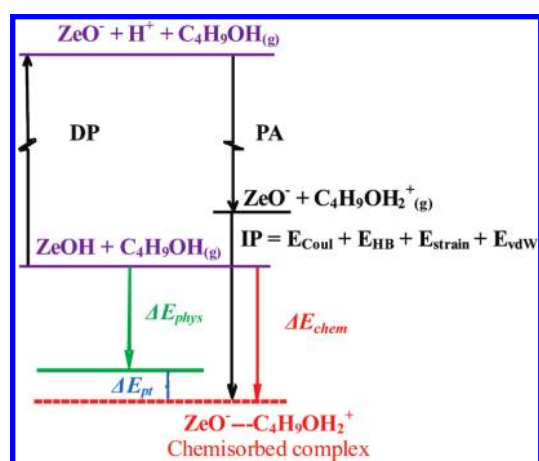
Figure 5. Energy levels corresponding to different interactions between the gas-phase butanol and zeolite.

Bader analysis allocated a total charge of +0.76 to +0.81 to the butoxonium fragments, which is in agreement with the range of +0.75 to +0.78 computed for oxonium species of C1−C3 primary alcohols.[18,25] Formal charges located on the O$_a$ and O$_b$ are identical for all butoxonium ions (Table 5), indicating that the charge allocation pattern is similar for all chemisorbed complexes. As a consequence of the complete proton transfer from the BAS to the butanol molecule, the zeolite framework is distorted to a greater extent as compared with that observed upon physisorption (Table 6).

3.3.2. Chemisorption Energy. The chemisorption energies of the butanols are shown in Table 7. At the straight channel, all butanols have comparable ΔE_{DFT-D} and largely similar ΔE_{DFT} and ΔE_D. At the zigzag channel, the ΔE_{DFT-D} strength decreases in going from 1-BuOH over 2-BuOH to i-BuOH and t-BuOH and broader ranges of ΔE_{DFT} and ΔE_D are observed.

Despite the difference in O−H bond length, significantly similar chemisorption energies are computed for t-butoxonium and t-butoxonium_sym at the straight channel as well as for 1-butoxonium and 1-butoxonium_sym at the zigzag channel (Table 7), revealing the very flat potential energy surfaces (PES) for the fluctuation of the O−H bonds of the oxonium ions.[18,25]

Assuming that the ion pair interactions (IPs) between the negatively charged zeolite and the protonated butoxonium ions mainly consist of stabilizing HB (E_{HB}), Coulomb (E_{Coul}), and vdW (E_{vdW}) interactions and destabilizing steric constraints (E_{strain}), an estimate of the stabilization of the gas phase butoxonium ions by the negatively charged zeolite (ZeO$^-$---C$_4$H$_9$OH$_2^+$) can be obtained based on the thermodynamic cycle presented in Figure 5. In this study, the same BAS site of H-ZSM-5 has been considered for all adsorption complexes and the deprotonation energy of 1236 kJ mol^{-1} as reported by Brand et al.[56] was used to calculate the IPs

$$IP_{DFT-D} = \Delta E_{DFT-D} - DP - PA$$
$$= E_{Coul} + E_{HB} + E_{vdW} + E_{strain} \quad (3)$$

$$IP_{DFT} = \Delta E_{DFT} - DP - PA = E_{Coul} + E_{HB} + E_{strain} \quad (4)$$

$$IP_D = IP_{DFT-D} - IP_{DFT} = \Delta E_D = E_{vdW} \quad (5)$$

At the straight channel, the total IP$_{DFT-D}$ strength decreases in the following order: 1-BuOH > i-BuOH > 2-BuOH > t-BuOH (Table 7) with increasing bulkiness of the butyl chain. For all butanols, the stabilizing vdW contribution, IP$_D$, is roughly the same and amounts to some −60 kJ mol^{-1}. In contrast, the DFT contribution, IP$_{DFT}$, decreases by 22−24 kJ mol^{-1} in going from 1-BuOH to t-BuOH, which can be mainly ascribed to the aforementioned increase in E_{strain} of 15 kJ mol^{-1} (Table 2) since all the butoxonium ions have rather similar structural parameters as well as formal charges and can thus be expected to have rather similar E_{HB} as well as E_{Coul} contributions.

At the zigzag channel, the decrease of 60 kJ mol^{-1} in IP$_{DFT}$ in going from 1-BuOH to t-BuOH can be mainly ascribed to the increase in E_{strain} of 63 kJ mol^{-1} (see Table 2). Despite the increase in IP$_D$ from −85 to −103 kJ mol^{-1}, the IP$_{DFT-D}$ follows the similar trend as the IP$_{DFT}$.

The differences in IP$_{DFT}$ and IP$_D$ contributions can also be used to rationalize the influence of the pore dimensions on the stability of the chemisorbed butoxoniums. Clearly, the interplay between steric constrains and vdW interactions accounts for the stronger chemisorption of 1-BuOH and 2-BuOH at the zigzag channel. The chemisorption of i-BuOH and t-BuOH is however

equally preferred by the straight and zigzag channels (see δ_{ch}-$[IP_{DFT}]$ and $\delta_{ch}[IP_D]$, Table 8).

3.3.3. Proton Transfer Energy. The very small proton transfer energies observed at the straight (0 to -3 kJ mol^{-1}) as well as at the zigzag ($+1$ to -4 kJ mol^{-1}) channel are indicative of the very flat potential energy surfaces for the proton transfer from the zeolite to the alcohols (see ΔE_{pt}, Table 7). Previous pbcDFT calculations also predicted very small energy differences between the protonated and hydrogen bonded complexes for a range of C1−C4 primary alcohols.[18,21,25] For the adsorption of methanol in zeolite, cluster calculations at the HF-SCF, MP2, and DFT levels of theory computed a broad and shallow potential energy surface that accommodates two equivalent neutral complexes with the ion-pair transition state connecting them.[15,16] It is apparent from the present periodic calculations that the physisorbed and chemisorbed complexes are the most stable species on the PES for the adsorption of butanols in H-ZSM-5 at 0 K The assumption of an equilibrium between these stable complexes is corroborated by the very small difference in energy between the physisorbed and chemisorbed complexes.

3.4. Stability of Adsorbed Complexes. Figure 6 represents the thermodynamic cycle for the formation of both physisorbed and chemisorbed complexes from the unloaded zeolite and the elements taken as the reference state, allowing a direct comparison of the stability of the adsorbed complexes of the different alcohols. The stabilization energy of the adsorbed complexes ($\Delta E_{phys,stab}$ or $\Delta E_{chem,stab}$) relative to the elements dependents on the standard enthalpy of formation, ΔH_f^0, of the gas-phase alcohol[57] and the adsorption energy (ΔE_{phys} or ΔE_{chem}) of the alcohol in H-ZSM-5

$$\Delta E_{phys,\,stab} = \Delta E_{phys} + \Delta H_f^0 \qquad (6)$$

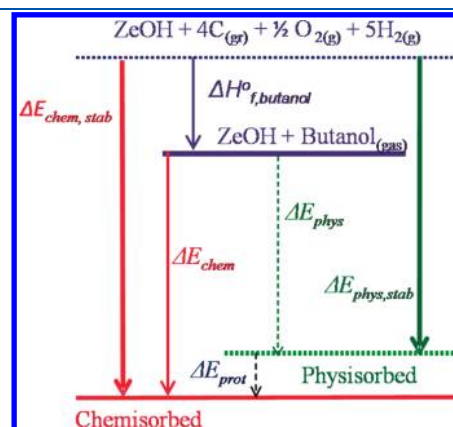$$\Delta E_{chem,\,stab} = \Delta E_{chem} + \Delta H_f^0 \qquad (7)$$

Table 9 presents the stabilization energy of all adsorbed complexes in H-ZSM-5. At the straight channel, the stability of both physisorbed and chemisorbed complexes increases in going from 1-BuOH over i-BuOH and 2-BuOH to t-BuOH. The largest difference in stability is observed between the 1-BuOH and t-BuOH chemisorbed complexes, amounting to 38 kJ mol^{-1} in favor of t-BuOH. At the zigzag channel, the stability of the adsorbed complexes increases in the following order: i-BuOH < 1-BuOH < 2-BuOH < t-BuOH.

3.5. Partial Hessian Vibrational Analysis. Three different interpretations[17] have been proposed to explain the experimentally observed triplet of bands at approximately 2800−3000, 2400−2600, and 1500−1700 cm^{-1} of alcohols adsorbed in several zeolites.[6−11] The first one assumes the formation of protonated alcohol (ROH_2^+) and assigns the three bands to the symmetric (ν_s) and asymmetric (ν_a) HOH stretch and (δ) HOH bending, respectively.[9,10] The second interpretation for the triplet is based on a Fermi resonance of the very broad $\nu(OH)$ stretch with the overtones of the in-plane $\delta_i(OH)$ and out-of-plane $\delta_o(OH)$ bending of zeolite in physisorbed complexes (Ze−OH---Y) such as the methanol-zeolite.[8] The last interpretation proposes an equilibrium between chemisorbed and physisorbed complexes (Ze−OH---Y $\leftrightarrow$ Ze-O$^-$---YH$^+$).[11] Given the very flat PES for the proton transfer, vibrations of the H_z proton in both the physisorbed and chemisorbed complexes are therefore to some extent characterized by anharmonicity.[18,20] Previous calculations[18,58,59] indicated that anharmonicity reduces the O_aH_z stretch of unloaded and loaded zeolites by 150−200 cm^{-1}. In the present work, vibrations of adsorbed complexes were analyzed within the harmonic approximation only since computation of anharmonic frequencies is not currently available within the VASP code. Harmonic frequencies

Table 8. Difference ($\delta_{ch}[\Delta E_{DFT-D}]$, kJ mol^{-1} = $\Delta E_{DFT-D}^{zigzag}$ − $\Delta E_{DFT-D}^{straight}$) in ΔE_{chem} and Difference (δ_{ch}, kJ mol^{-1} = IP^{zigzag} − $IP^{straight}$) in IP Energies Computed between the Zigzag and Straight Channel of H-ZSM-5 Obtained Using the pbc[DFT-D] Approach

	ΔE_{chem}	IP		
	$\delta_{ch}[\Delta E_{DFT-D}]$	$\delta_{ch}[IP_{DFT-D}]$	$\delta_{ch}[IP_{DFT}]$	$\delta_{ch}[IP_D]$
1-BuOH	−14	−14	+5	−19
i-BuOH	+1	+1	+37	−36
2-BuOH	−11	−11	+27	−38
t-BuOH	+2	+2	+41	−39

Figure 6. Stability of physisorbed and chemisorbed complexes relative to the elements.

Table 9. Stability of Physisorbed and Chemisorbed BuOH-H-ZSM-5 Complexes Relative to the Elements

	straight channel		zigzag channel		
	$\Delta E_{phys} + \Delta H_f^0$	$\Delta E_{chem} + \Delta H_f^0$	$\Delta E_{phys} + \Delta H_f$	$\Delta E_{chem} + \Delta H_f^0$	ΔH_f^{0a}
1-BuOH	−423	−425	−435	−439	−275
i-BuOH	−431	−431	−431	−430	−284
2-BuOH	−437	−438	−448	−450	−293
t-BuOH	−460	−463		−460	−312

^{a} Standard formation enthalpies (kJ mol^{-1}) of the gas-phase alcohols taken from ref 57.

8666

dx.doi.org/10.1021/jp111698b |*J. Phys. Chem. C* 2011, 115, 8658–8669

Table 10. Selected Harmonic Vibrational Frequencies $(cm^{-1})^a$ for Unloaded H-ZSM-5, Gas-Phase Butanols, and the Most Stable Physisorbed Complexes of Butanols in H-ZSM-5 Obtained Using the pbc[DFT-D] Approach[b]

	$\nu(CH)$	$\delta(CH)$	$\delta(CH_3)$	$\nu(OH)$	$\nu(O_aH_z)^c$	$\delta_i(O_aH_z)^c$	$\delta_o(O_aH_z)$
H-ZSM-5					3737	1110	353
1-BuOH							
gas phase	2896−3035	1427−1464	1351	3759			
2HB_zig_O$_a$H$_z$	2964−3067	1427−1460	1350	3425	1392	1669	1171
i-BuOH							
gas phase	2892−3056	1423−1454	1349	3757			
2HB_str_O$_a$H$_z$	2945−3057	1426−1458	1366	3497	1403	1647	1187
2-BuOH							
gas phase	2882−3046	1408−1445	1348	3743			
2HB_zig_O$_a$H$_z$	2956−3108	1415−1454	1374	3427	1370	1717	1203
t-BuOH							
gas phase	2942−3053	1405−1450	1355	3696			
2HB_str_O$_a$H$_z$	2961−3077	1414−1455	1375	3368	1478	1757	1203

[a] Atom labels are defined in Figure 3. [b] ν, stretching mode; δ, bending mode; $\delta_i(O_aH_z)$ in-plane and $\delta_o(O_aH_z)$ out-of-plane bending modes of the zeolite O_aH_z. [c] $\nu(O_aH_z)$ and $\delta_i(O_aH_z)$ are coupled with $\nu(OH_z)$ and $\delta(OH_z)$, respectively.

Table 11. Selected Harmonic Vibration Frequencies $(cm^{-1})^a$ for the Most Stable Chemisorbed Complexes of Butanols in H-ZSM-5 Obtained Using the pbc[DFT-D] Approach[b]

	$\nu(CH)$	$\delta(CH)$	$\delta(CH_3)$	$\nu_s(HOH_z)$	$\nu_a(HOH_z)$	$\delta(HOH_z)$
1-butoxonium_zig	2965−3082	1423−1452	1357	2669	2243	1642
1-butoxonium_zig_sym	2967−3080	1423−1452	1356	2603	2319	1643
i-butoxonium_str	2947−3060	1419−1447	1373	2666	2292	1628
2-butoxonium_zig	2985−3086	1420−1444	1358	2671	2459	1634
t-butoxonium_str	2966−3068	1413−1456	1377	2812	2325	1626
t-butoxonium_str_sym	2964−3068	1413−1457	1375	2711	2434	1635

[a] Atom labels are defined in Figure 4. [b] ν, stretching mode; δ, bending mode; ν_s; symmetric stretching mode; v_a, asymmetric stretching mode.

reported here provide a qualitative agreement with the experimental IR data.

Selected harmonic frequencies of the most stable physisorbed and chemisorbed complexes, that is, 2HB_zig_O$_a$H$_z$ and butoxonium_zig of 1-BuOH and 2-BuOH together with 2HB_str_O$_a$H$_z$ and butoxonium_str of i-BuOH and t-BuOH are presented in Tables 10 and 11. For a complete discussion on harmonic vibrations of butanol isomers adsorbed in H-ZSM-5, see the Supporting Information (S7). Assuming an equilibrium between the physisorbed and chemisorbed complexes, the three much debated IR regions of the four butanols[27−31] can be explained. The first region, 2800−3000 cm^{-1}, corresponds solely to the $\nu(CH)$ stretching (2945−3108 cm^{-1}, Tables 10 and 11) of both physisorbed and chemisorbed complexes. The broad bands in the second region 2000−2700 cm^{-1}, can be assigned to the symmetric $\nu_s(HOH_z)$ and asymmetric $\nu_a(HOH_z)$ stretching modes of the chemisorbed complexes. The third region, centered around 1500−1600 cm^{-1}, may be attributed to the chemisorbed $\delta(HOH_z)$ and physisorbed in plane $\delta_i(O_aH_z)$ bending modes. The observed IR regions[27−31] for $\delta(CH_3)$ at 1380−1391 cm^{-1} and $\delta(CH)$ at 1446−1470 cm^{-1} find a good agreement with the calculated values (1380−1391 and 1446−1470 cm^{-1} for respective $\delta(CH_3)$ and $\delta(CH)$, Tables 10 and 11). The highest frequency band around 3500−3700 cm^{-1} observed for i-BuOH and t-BuOH in H-ZSM-5[30,31] can be assigned to the $\nu(OH)$ of the 2-HB physisorbed complexes (3368−3497 cm^{-1}) and/or to the $\nu(O_aH_z)$ of free BAS (3737 cm^{-1}).

4. CONCLUSIONS

The results reported here demonstrate that the pbc[DFT-D] approach is an efficient method for obtaining detailed information on the structure and energy of alcohols adsorbed in H-ZSM-5 zeolite, taking into account both bonded and nonbonded interactions. Having dimensions comparable to the channel's diameter of H-ZSM-5, the four butanols prove to be very useful probe molecules to evaluate the influence of the pore structure and size effects of the H-ZSM-5 framework.

The effect of the zeolite framework on the physisorption of the isomeric butanols results from an interplay of steric constraints, vdW dispersive interactions and hydrogen bonding between the BAS and the alcohol. In essence, steric constraints destabilize the alcohol−zeolite interaction and have a pronounced influence at the more confined zigzag channel, especially for the branched alcohols. In contrast, the dispersive vdW interactions contribute to the stabilization of the butanols inside the zeolite pores and fully counterbalance or even overweighs the steric constraints. The strength of the hydrogen bonding increases with increasing PA of the alcohol. Consequently, the physisorption of i-BuOH and t-BuOH is equally preferred by the zigzag and straight

channels while 1-BuOH and 2-BuOH favorably physisorb at the zigzag channel. For chemisorptions, the same preference as for physisorption results from an interplay between the steric constrains and dispersive vdW interactions since Coulomb and hydrogen bonding interactions are similar for the four isomeric butoxonium ions.

The concept of an equilibrium between the physisorbed and chemisorbed minima is corroborated by a very delicate difference in energy between them. It explains the experimental IR spectra of the four butanols adsorbed in H-ZSM-5.

■ ASSOCIATED CONTENT

ⓢ **Supporting Information.** Geometrical illustrations of butanols adsorbed in silicalite and H-ZSM-5 are given. Performance of pbcDFT + D versus pbc[DFT-D] with respect to geometries, adsorption energies, and vibrational frequencies of adsorbed complexes is detailed. Also, geometrical parameters and adsorption energies of butanols physisorbed over the BAS $O_aAl[O_bH_z]$ are presented. This material is available free of charge via the Internet at http://pubs.acs.org.

■ AUTHOR INFORMATION

Corresponding Author
*Tel: +32 (0)9 264 4516. Fax: +32 (0)9 264 4999. E-mail: MarieFrancoise.Reyniers@ugent.be.

■ ACKNOWLEDGMENT

■ REFERENCES

(1) Smith, J. V. *Chem. Rev.* **1988**, *88*, 149–182.
(2) Smit, B.; Maesen, T. L. M. *Chem. Rev.* **2008**, *108*, 4125–4184.
(3) Corma, A.; Iborra, S.; Velty, A. *Chem. Rev.* **2007**, *107*, 2411–2502.
(4) Huber, G. W.; Corma, A. *Angew. Chem., Int. Ed.* **2007**, *46*, 7184–7201.
(5) Huber, G. W.; Iborra, S.; Corma, A. *Chem. Rev.* **2006**, *106*, 4044–4098.
(6) Aronson, M. T.; Gorte, R. J.; Farneth, W. E. *J. Catal.* **1987**, *105*, 455–468.
(7) Aronson, M. T.; Gorte, R. J.; Farneth, W. E. *J. Catal.* **1986**, *98*, 434–443.
(8) Kotrla, J.; Nachtigallová, D.; Kubelková, L.; Heeribout, L.; Doremieux-Morin, C.; Fraissard, J. *J. Phys. Chem. B* **1998**, *102*, 2454–2463.
(9) Izmailova, S. G.; Karetina, I. V.; Khvoshchev, S.; Shubaeva, M. A. *J. Colloid Interface Sci.* **1994**, *165*, 318–324.
(10) Mirth, G.; Lercher, J. A.; Anderson, M. W.; Kinowski, J. *J. Chem. Soc., Faraday Trans.* **1990**, *86*, 3039–3044.
(11) Kubelková, L.; Nováková, J.; Nedomová, K. *J. Catal.* **1990**, *124*, 441–450.
(12) van Santen, R. A. *Catal. Today* **1997**, *38*, 377–390.
(13) van Santen, R. A.; Kramer, G. J. *Chem. Rev.* **1995**, *95*, 637–660.
(14) Sauer, J.; Ugliengo, P.; Garrone, E.; Saunders, V. R. *Chem. Rev.* **1994**, *94*, 2095–2160.
(15) Haase, F.; Sauer, J. *J. Am. Chem. Soc.* **1995**, *117*, 3780–3789.

(16) Blaszkowski, S. R.; van Santen, R. A. *J. Phys. Chem.* **1995**, *99*, 11728–11738.
(17) Pelmenschikov, A. G.; van Wolput, J. H. M. C.; Jänchen, J.; van Santen, R. A. *J. Phys. Chem.* **1995**, *99*, 3612–3617.
(18) Shah, R.; Gale, J. D.; Payne, M. C. *J. Phys. Chem.* **1996**, *100*, 11688–11697.
(19) Haase, F.; Sauer, J.; Hutter, J. *Chem. Phys. Lett.* **1997**, *266*, 397–402.
(20) Stich, I.; Gale, J. D.; Terakura, K.; Payne, M. C. *Chem. Phys. Lett.* **1998**, *283*, 402–408.
(21) Haase, F.; Sauer, J. *Microporous Mesoporous Mater.* **2000**, *35−36*, 379–385.
(22) Svelle, S.; Tuma, C.; Rozanska, X.; Kerber, T.; Sauer, J. *J. Am. Chem. Soc.* **2009**, *131*, 816–825.
(23) Derouane, E. G. *J. Mol. Catal. A: Chem.* **1998**, *134*, 29–45.
(24) Stich, I.; Gale, J. D.; Terakura, K.; Payne, M. C. *J. Am. Chem. Soc.* **1999**, *121*, 3292–3302.
(25) Nguyen, C. M.; Reyniers, M. F.; Marin, G. B. *Phys. Chem. Chem. Phys.* **2010**, *12*, 9481–9493.
(26) Lee, C. C.; Gorte, R. J.; Farneth, W. E. *J. Phys. Chem. B* **1997**, *101*, 3811–3817.
(27) Makarova, M. A.; Paukshtis, E. A.; Thomas, J. M.; Williams, C.; Zamaraev, K. I. *J. Catal.* **1994**, *149*, 36–51.
(28) Makarova, M. A.; Williams, C.; Zamaraev, K. I. *J. Chem. Soc., Faraday Trans.* **1994**, *90*, 2147–2153.
(29) Makarova, M. A.; Williams, C.; Romannikov, V. N.; Zamaraev, K. I. *J. Chem. Soc., Faraday Trans.* **1990**, *86*, 581–584.
(30) Williams, C.; Makarova, M. A.; Malysheva, L. V.; Paukshtis, E. A.; Zamaraev, K. I. *J. Chem. Soc., Faraday Trans.* **1990**, *86*, 3473–3485.
(31) Williams, C.; Makarova, M. A.; Malysheva, L. V.; Paukshtis, E. A.; Talsi, E. P.; Thomas, J. M.; Zamaraev, K. I. *J. Catal.* **1991**, *127*, 377–392.
(32) Shubin, A. A.; Catlow, C. R. A.; Thomas, J. M.; Zamaraev, K. I. *Proc.−R. Soc., Sect. A: Math. Phys. Sci.* **1994**, *446*, 411–427.
(33) Kerber, T.; Sierka, M.; Sauer, J. *J. Comput. Chem.* **2008**, *29*, 2088–2097.
(34) Grimme, S. *J. Comput. Chem.* **2006**, *27*, 1787–1799.
(35) Sklenak, S.; Dedecek, J.; Li, C.; Wichterlova, B.; Gabova, V.; Sierka, M.; Sauer, J. *Phys. Chem. Chem. Phys.* **2009**, *11*, 1237–1247.
(36) Gabova, V.; Dedecek, J.; Cejka, J. *Chem. Commun.* **2003**, *10*, 1196–1197.
(37) Schroder, K. P.; Sauer, J.; Leslie, M.; Richard, C.; Catlow, C. R. A. *Zeolites* **1992**, *12*, 20–23.
(38) Nachtigallova, D.; Nachtigall, P.; Sierka, M.; Sauer, J. *Phys. Chem. Chem. Phys.* **1999**, *1*, 2019–2026.
(39) Sazama, P.; Dedecek, J.; Gabova, V.; Wichterlova, B.; Spoto, G.; Bordiga, S. *J. Catal.* **2008**, *254*, 180–189.
(40) Alvarado-Swaisgood, A. E.; Barr, M. K.; Hay, P. J.; Redondo, A. *J. Phys. Chem.* **1991**, *95*, 10031–10036.
(41) Brändle, M.; Sauer, J. *J. Am. Chem. Soc.* **1998**, *120*, 1556–1570.
(42) Jungsuttiwong, S.; Limtrakul, J.; Truong, T. N. *J. Phys. Chem. B* **2005**, *109*, 13342–13351.
(43) Clark, L. A.; Sierka, M.; Sauer, J. *J. Am. Chem. Soc.* **2004**, *126*, 936–947.
(44) Zamaraev, K. I.; Thomas, J. M. *Adv. Catal.* **1996**, *41*, 335–358.
(45) Henkelman, G.; Arnaldsson, A.; Jónsson, H. *Comput. Mater. Sci.* **2006**, *36*, 354–360.
(46) (a) Kresse, G.; Hafner, J. *Phys. Rev. B* **1993**, *48*, 13115–13118. (b) Kresse, G.; Hafner, J. *Phys. Rev. B* **1994**, *49*, 14251–14269. (c) Kresse, G.; Furthmuller, J. *Computat. Mater. Sci.* **1996**, *6*, 15–50. (d) Kresse, G; Furthmuller, J. *Phys. Rev. B* **1996**, *54*, 11169–11186.
(47) Blochl, P. E. *Phys. Rev. B* **1994**, *50*, 17953.
(48) Kresse, G.; Joubert, D. *Phys. Rev. B* **1999**, *59*, 1758.
(49) Perdew, J. P.; Burke, K.; Ernzerhof, M. *Phys. Rev. Lett.* **1996**, *77*, 3865–3868.
(50) Ewald, P. *Ann. Phys.* **1921**, *369*, 253–287.
(51) Holmes, J. L.; Aubry, C.; Mayer, P. M. *J. Phys. Chem. A* **1999**, *103*, 705–709.

8668

dx.doi.org/10.1021/jp111698b |*J. Phys. Chem. C* 2011, 115, 8658–8669

(52) Hunter, E.; Lias, S. *J. Phys. Chem. Ref. Data* **1998**, *27*, 413–656.

(53) Pau, J. K.; Kim, J. K.; Caserio, M. C. *J. Am. Chem. Soc.* **1978**, *100*, 3831–3837.

(54) Wolf, J. F.; Staley, R. H.; Taagepera, M.; McIver, R. T.; Beauchamp, J. L., Jr.; Taft, R. W. *J. Am. Chem. Soc.* **1977**, *99*, 5417–5429.

(55) Benoit, F. M.; Harrison, A. G. *J. Am. Chem. Soc.* **1977**, *99*, 3980–3984.

(56) Brand, H. V.; Curtiss, L. A.; Iton, L. E. *J. Phys. Chem.* **1993**, *97*, 12773–12782.

(57) http://webbook.nist.gov/chemistry/ (accessed Mar 22, 2011).

(58) Sastre, G.; Katada, N.; Suzuki, K.; Niwa, M. *J. Phys. Chem. C* **2008**, *112*, 19293–19301.

(59) Vener, M. V.; Rozanska, X.; Sauer, J. *Phys. Chem. Chem. Phys.* **2009**, *11*, 1702–1712.

8669

dx.doi.org/10.1021/jp111698b |*J. Phys. Chem. C* 2011, 115, 8658–8669